A Novel Hollow-Fiber Reactor with Reversible Immobilization of Lactase

Experimental and theoretical studies on a backflush hollow-fiber enzymatic reactor (HFER) were conducted in this work for a lactose/lactase system. An *A. niger* lactase was chosen, from the four lactases tested, for reversible immobilization in the sponge layers of the fibers. An enzyme loading procedure was developed that allowed reliable and reproducible operation of the hollow-fiber reactor and produced industrially significant conversions without apparent change in the activity or stability of the lactase used. This reversible immobilization scheme also permitted easy replacement of the enzyme used. The performance of the backflush HFER was investigated and a large number of data concerning its operation were obtained and interpreted. Momentum and mass transports in such a HFER were analyzed, and mathematical models that took the experimental findings into consideration were also developed and solved analytically and/or numerically. Predictions from the computer model developed in this work were found to be in excellent agreement with the experimental data collected, suggesting the possibility of *a priori* design of a process-scale backflush HFER. With minor modifications, the models developed are expected to be applicable to hollow-fiber reactors with a wide selection of immobilized cells, organelles, and other enzymes.

C. K. S. Jones, R. Y. K. Yang, E. T. White
Department of Chemical Engineering
University of Queensland
St. Lucia, QLD 4067 Australia

Introduction

A large number of enzyme immobilization schemes involve chemical coupling of enzymes to a solid support. In addition to chemical binding, physical techniques such as adsorption, gel entrapment, and encapsulation have been used. Enzymes immobilized by encapsulation usually can expect to experience an environment similar to that of free enzymes in an aqueous solution. In particular, if the enzyme is encapsulated after the formation of an encapsulating medium, it should retain its intrinsic kinetic properties.

Examples of the last method of immobilization are the hollow-fiber enzymatic reactor (HFER) investigated by Breslau and Kilcullen (1975), Robertson et al. (1976), Rony (1971), and Waterland et al. (1974, 1975). All these reactors allow the enzymes to be truly immobilized under mild conditions without causing alteration of their inherent kinetic behaviors. However, with the notable exception of the first work, all these reactor schemes relied solely on diffusion as the means of contacting substrates and enzymes.

Breslau and Kilcullen have suggested a number of HFER's in which the bulk flow is an important transport mechanism. Of great interest is the backflush mode of operating a HFER, in which substrates flow from the shell of a hollow-fiber cartridge to the lumina of the fibers, and enzymes are loaded into the sponge layers of the anisotropic membranes simply by backflushing (flowing from shell to lumen) the reactor with a solution of the enzyme to be immobilized. Backflushing is illustrated in Figure 1a. The extrathin membrane retains the enzyme while allowing the solvent, the products, and the unreacted reactants to pass through to the fiber lumen and flow out of the reactor. This method of enzyme loading has also been adopted by Korus and Olson (1977) and Pedersen et al. (1978).

The backflush HFER, that is, a HFER operated in backflush mode, is the simplest way of operating a hollow-fiber reactor containing enzyme in the sponge layer that is not permanently fixed. The enzyme in the sponge region is immobilized in the

Correspondence concerning this paper should be addressed to R. Y. K. Yang, whose current address is Department of Chemical Engineering, West Virginia University, Morgantown, WV 26506-6101.

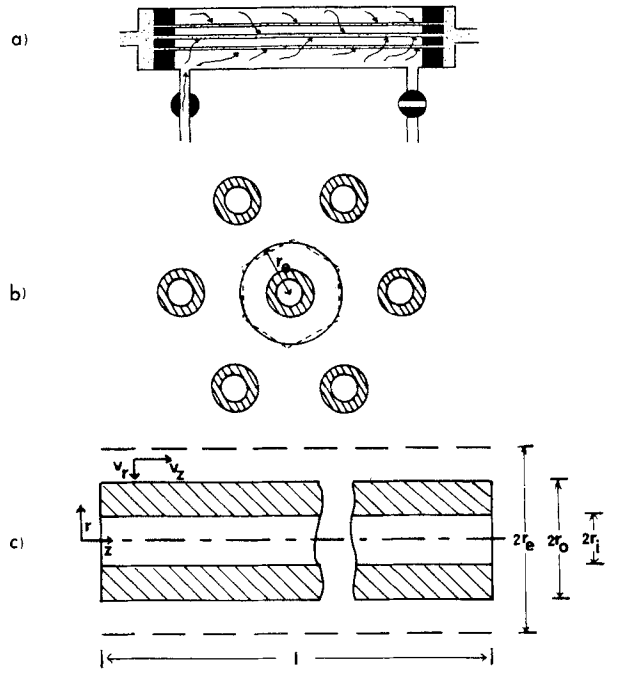

Figure 1a. Hollow-fiber reactor in backflush mode.
b. Cross section: hollow fibers in equilateral triangle array.
c. Representative hollow fiber and surroundings.

sense that it is retained by the thin membrane with suitable molecular weight cutoff and cannot enter the fiber lumen. The enzymes so immobilized can be washed out easily for replacement by simply reversing the direction of bulk flow in the reactor, thus achieving reversible immobilization of enzymes.

The procedure for optimal enzyme loading and the performance of a backflush HFER with reversible immobilization of lactase were investigated experimentally in this work. Extremely high enzyme loading density and thus significantly high substrate conversion were achieved. A large number of experimental data associated with the performance of the reactor were obtained, and it was found that enzyme loading, flow rate, and feed concentration affected the conversion of lactose in a complex relationship. Furthermore the performance of the reactor was found to fall invariably between that expected for a plug-flow tubular reactor and that for a continuous stirred-tank reactor.

In addition to the experimental work conducted, momentum and mass transports in a backflush HFER were also analyzed and mathematical models were developed to describe the velocity and concentration profiles in such a reactor. Theoretical predictions based on numerical as well as analytical solutions of the models were found to be in good agreement with the experimental data obtained.

A major conclusion of practical importance that emerges from this investigation is that, using the enzyme loading procedure and the reactor operating strategy established here, properly chosen enzyme can be reversibly immobilized in a commercially available hollow-fiber cartridge to achieve reliable and reproducible operation of the reactor and obtain industrially significant conversion without major alterations of enzyme activity, stability, and other kinetic properties. Once deactivated after a period of continuous operation, the enzyme can be flushed out easily by simply reversing the flow direction in the cartridge, and the reactor will then be ready for reloading a new batch of fresh enzyme.

The use of the backflush HFER is currently limited by two considerations:

1. The feed must be of permeate quality in order to ensure that particulates do not plug or damage the extrathin fiber membrane
2. The flow rate must not be so high as to allow the pressure drop across the membrane to exceed the burst strength of the fibers

These limitations are not of major concern in many enzyme-catalyzed reactions, since high-pressure differentials cannot be tolerated by most enzymes anyway, and in many industrial applications of enzymes, the product must be of permeate quality. Furthermore, recent developments in polymer processing may quickly eliminate the problem concerning the burst strength of the fibres.

Model Development

There is no record in the literature of previous attempts to mathematically model the performance of a backflush HFER. Researchers who previously studied HFER's used them in such a way that there was either no convective flow through the fiber sponge or the fluid had a constant flow rate in the lumen.

In this work, it is assumed that the fibers in the cartridge are arranged in a regular pattern, namely, an equilateral triangular pitch as shown in Figure 1b, although they are positioned in a random manner. This simplification has been adopted by a number of workers for related problems, including Gill and Bansal (1973) and Noda and Gryte (1979). Since the number of fibers involved is large, the effect of the shell wall on each fiber may be neglected. In addition, due to the symmetric property of the equilateral triangular array, only a single fiber needs to be considered. A typical fiber and its surroundings, which is the basis of model development in this section, is shown in Figure 1c. Note that the positive z direction is taken to be in the direction of axial flow in the lumen, while the positive radial direction is outward.

Since each fiber is equidistant from six neighboring fibers, we would ideally expect a hexagonal free-shear surface to surround each fiber. Because variations in concentration and pressure are small around the periphery of this hexagonal boundary, it is replaced with a circular boundary having the same area between the shear-free hexagonal boundary and the fiber wall, as shown in Figure 1b. This allows us to define an equivalent radius r_e based on the outside fiber radius and the void fraction of the reactor (not occupied by fibers), that is:

$$r_e \triangleq \left(\frac{1}{1-\epsilon}\right)^{1/2} r_o \tag{1}$$

The assumption of a shear-free surface around each fiber also leads to peripheral symmetry and the absence of angular component of velocity.

Only steady state operation of the reactor is considered. In consistence with the experimental conditions employed in this study, we also neglect osmotic effects and assume:

1. Constant temperature throughout the reactor

2. Newtonian fluid with constant physical properties
3. Negligible change in the kinetic properties of immobilized enzymes

Furthermore, we assume that momentum balance equations and mass balance equations are not coupled and may be solved separately. This simplification is reasonable if the velocity of the fluid is independent of concentrations and the process is carried out isothermally.

We begin with a description of the velocity and concentration profiles within the three regions—shell, sponge, and lumen—of a backflush HFER.

Velocity distribution

In many respects the backflush HFER has a velocity profile similar to that of the hollow-fiber reverse-osmosis system investigated by Gill and Bansal (1973) and Doshi et al. (1977). Hence, the approach used by Gill and coworkers is adopted in this section with due consideration to the differences between the systems. These differences are that, for a HFER:

1. Fluid does not leave through the shell side
2. Lower pressures are involved
3. Velocity profiles are independent of concentration profiles

Thus, the momentum balance equations and the associated boundary conditions for the three regions of a representative hollow fiber in the backflush HFER are the same as Eqs. 1–3, 5, 7, 8, and 10 of Gill and Bansal. Those coupled partial differential equations (PDE's) and their boundary conditions, in the context of a HFER, imply that the feed solution enters the shell region of the fiber at $z = 0$ with a fully developed velocity profile. Both axial and radial components of flow in the shell are considered, but the flow parallel to the fibers is laminar. The flow in the sponge region is assumed to be in the radial direction only. Although it totally retains the enzyme, the extrathin membrane at the inner fiber wall is also assumed to provide negligible resistance to the passage of substrates or products. Similar to the shell-side flow, both axial and radial flows in the lumen are considered and the flow in the axial direction is that of a well-developed laminar flow.

For the shell region, the PDE's and the associated boundary conditions can be reduced to a much simpler ordinary differential equation (ODE) in terms of a dimensionless area-averaged axial velocity u_{1m}, following the same approach as that of Gill and Bansal but omitting the osmotic pressure and concentration effects.

The simplified relations are

$$\frac{d^2u_{1m}}{d\zeta^2} = u_{1m} \tag{2a}$$

with $u_{1m}(0) = 1$ and $u_{1m}\ (\eta\ell/r_o) = 0$ for countercurrent flow, and

$$\frac{d^2u_{1m}}{d\zeta^2} = u_{1m} - b \tag{2b}$$

with $u_{1m}(0) = 1$ and $u_{1m}\ (\eta\ell/r_o) = 0$ for cocurrent flow, where the two dimensionless groups involved are

$$\eta \triangleq \left(\frac{2A\mu\alpha r_o}{r_e^2 - r_o^2} + \frac{16A\mu r_o^3}{r_i^4}\right)^{1/2}, \quad b \triangleq \left[1 + \frac{\alpha r_i^4}{8r_o^2(r_e^2 - r_o^2)}\right]^{-1} \tag{2c}$$

and the dimensionless variable $\zeta \triangleq \eta z/r_o$. It should be noted that these equations are in the form of a two-point boundary value problem, while the equivalent equations obtained by Gill and Bansal are in the form of an initial-value problem. This is a reflection of the fact that there is no flow out of the shell of the backflush HFER modeled here.

Equation 2 can be solved readily to obtain the following expressions for the mean axial velocity in the shell:

$$v_{z_{1m}}(z) = v_{z_{1m}}(0)\left[\exp\left(\eta\frac{z}{r_o}\right) - \exp\left(\eta\frac{\ell}{r_o}\right)\frac{\sinh\left(\eta\dfrac{z}{r_o}\right)}{\sinh\left(\eta\dfrac{\ell}{r_o}\right)}\right] \tag{3a}$$

for countercurrent flow, and

$$v_{z_{1m}}(z) = v_{z_{1m}}(0) \cdot \left(b\left\{1 - \exp\left(\eta\frac{z}{r_o}\right) - \frac{\sinh\left(\eta\dfrac{z}{r_o}\right)}{\sinh\left(\eta\dfrac{\ell}{r_o}\right)}\left[1 - \exp\left(\eta\frac{\ell}{r_o}\right)\right]\right\} + \exp\left(\eta\frac{z}{r_o}\right) - \exp\left(\eta\frac{\ell}{r_o}\right)\frac{\sinh\left(\eta\dfrac{z}{r_o}\right)}{\sinh\left(\eta\dfrac{\ell}{r_o}\right)}\right) \tag{3b}$$

for cocurrent flow.

This velocity can be related to the radial wall velocity $v_{rw}(z)$ by carrying out a differential momentum balance over a small length Δz of the shell region to yield

$$\frac{dv_{z_{1m}}(z)}{dz} = \frac{2r_o v_{rw}(z)}{(r_e^2 - r_o^2)} \tag{4}$$

or

$$v_{z_{1m}}(z) = v_{z_{1m}}(0) + \frac{2r_o}{r_e^2 - r_o^2}\int_o^z v_{rw}(z')\,dz' \tag{5}$$

Equation 4 can be used together with Eq. 3 to obtain $v_{rw}(z)$. Alternatively, one can further employ Eq. 5 to obtain an area-averaged radial wall velocity between any two positions z_1 and z_2 in the axial direction, namely,

$$\bar{v}_{rw} \triangleq \frac{\int_{z_1}^{z_2} v_{rw}(z')\,dz'}{z_2 - z_1}, \quad \ell \geq z_2 \geq z_1 \geq 0 \tag{6}$$

Soltanieh and Gill (1981) have reviewed transport models for reverse-osmosis membranes and concluded that solvent (water) flux can adequately be described by a simple solution-diffusion model:

$$v_{rw}(z) = -A[P_{1w}(z) - P_{3w}(z)] \tag{7}$$

This relation allows us to relate the wall velocity to the pressure drop across the sponge region, with the membrane coefficient A serving as the solvent permeability coefficient and taking care of the effect of both the membrane and the enzyme.

Significant simplification of the analysis of velocity profile is possible if we assume that the shell-side pressure is constant (Doshi et al., 1977). This is a reasonable assumption if the flow rate is small and flow area is large, which is the condition likely to be associated with a backflush HFER. In this case Eq. 7 becomes

$$v_{rw}(z) = -A[P_1 - P_3(z)] \tag{8}$$

where P_1 is the uniform pressure throughout the shell region and P_3 is independent of r.

The Hagen-Poiseuille equation for flow inside a pipe may be used in the lumen to get

$$\frac{dP_3}{dz} = -\frac{8\mu}{r_i^2} v_{z_{3m}}(z) \tag{9}$$

where it is recognized that $v_{z_{3m}}$ varies with axial position (Dandavati et al., 1975). Equation 9, when combined with a differential momentum balance over a small length of the lumen, gives

$$\frac{dP_3}{dz} = \frac{16\mu r_o}{r_i^4}\int_o^z v_{rw}(z')\,dz' = -\frac{\beta^2}{\ell^2}\int_o^z [P_1 - P_3(z')]\,dz',\ \ell \geq z \geq 0 \tag{10}$$

where

$$\beta^2 \triangleq 16\mu r_o A\ell^2/r_i^4.$$

The hollow fibers are potted in an epoxy seal of about 10 mm length at both ends of the cartridge, as represented by the black bands in Figure 1a. At the inlet end of the reactor there is no flow through the lumen, so the seal at this end may be neglected. However, at the exit end, since there is no radial flow through the fibers over the length of the seal ℓ_s, the pressure drop is constant in the region between ℓ and $\ell + \ell_s$ and is given by

$$\frac{dP_3}{dz} = -\frac{\beta^2}{\ell^2}\int_{\ell}^{\ell+\ell_s} [P_1 - P_3(z')]\,dz' \triangleq -\delta \tag{11}$$

Hence we have

$$P_3(z) = P_{ex} + \delta(\ell + \ell_s - z),\ \ell + \ell_s \geq z \geq \ell \tag{12}$$

where P_{ex} is the pressure at the lumen exit, that is, at $z = \ell + \ell_s$.

Differentiation of Eq. 10 with respect to z yields a second-order ODE, which can be solved to obtain

$$P_1 - P_3(z) = \frac{\Delta P}{\cosh\beta + \left(\frac{\ell_s}{\ell}\right)\beta\sinh\beta}\cosh\left(\frac{\beta z}{\ell}\right) \tag{13}$$

by satisfying the boundary condition

$$\frac{dp_3(z)}{dz} = 0 \quad \text{at } z = 0$$

and also Eq. 12 at $z = \ell$. Note that $\Delta P \triangleq P_1 - P_{ex}$ is the pressure difference between the inlet and the outlet of the backflush HFER.

Hence we also obtain the following expression, which relates the radial wall velocity to ΔP:

$$v_{rw}(z) = \frac{-A\Delta P\cosh\left(\frac{\beta z}{\ell}\right)}{\cosh\beta + \left(\frac{\ell_s}{\ell}\right)\beta\sinh\beta} \tag{14}$$

The corresponding mean radial wall velocity between z_1 and z_2 is

$$\bar{v}_{rw} = \frac{-\frac{A\ell}{\beta}\Delta P\left[\sinh\left(\frac{\beta z_2}{\ell}\right) - \sinh\left(\frac{\beta z_1}{\ell}\right)\right]}{\left[\cosh\beta + \left(\frac{\ell_s}{\ell}\right)\beta\sinh\beta\right](z_2 - z_1)},\ \ell \geq z_2 \geq z_1 \geq 0 \tag{15}$$

Using the above two expressions, various axial and radial components of the velocity as functions of z and/or r, as well as $v_{z_{1m}(z)}$ and $v_{z_{3m}(z)}$, were also obtained (Jones, 1983). However, it is the expressions for the radial wall velocity that are of prime interest to the performance of a backflush HFER.

Concentration distribution

We have found in our laboratory that it is relatively easy to operate the backflush HFER with the shell region totally free of enzymes. With no possibility for enzymatic reactions to occur, it is reasonable to assume that substrate concentration is uniform throughout the shell region. As it is unlikely to have any concentration polarization of substrate or product in the lumen, the only source of concentration variation in the reactor is enzymatic reaction in the sponge region, where the enzyme is assumed to be distributed evenly over the entire depth of the sponge layer. It is further assumed that there is no adsorption of either substrate or product by the sponge layer, which is confirmed in this work for the lactase/lactose system investigated. To simplify the model, dispersion along the axial direction of the hollow-fiber cartridge is also neglected in all regions of the reactor.

Equation 14 indicates that radial wall velocity is a weak function of axial position z. Experimental observations further suggest that the radial wall velocity may be taken as being constant under the experimental conditions of this work. This allows us to further assume that the concentrations in the lumen are independent of z. Thus, the axial dependence of concentrations is removed from consideration and we need only solve the coupled substrate and product balances in the sponge region of the fiber. These balances take the form of two simultaneous second-order boundary value type ODE's. Without these simplifications, the general material balances for substrate and product would have led to a set of six coupled second-order PDE's.

The most suitable model for both substrate and product con-

centrations in the sponge layer are simply the "axial" dispersion plug-flow reactor model in which the axis of the "reactor is" the radial direction of the fiber, that is,

$$D_s \frac{d^2s}{dr^2} + \frac{1}{r}(D_s - v_{rw}r_o)\frac{ds}{dr} - f(s,p) = 0 \qquad (16)$$

$$D_p \frac{d^2p}{dr^2} + \frac{1}{r}(D_p - v_{rw}r_o)\frac{dp}{dr} + f(s,p) = 0 \qquad (17)$$

where, for competitive product-inhibition type enzymatic reactions, such as that associated with the lactase/lactose system,

$$f(s,p) = \frac{kEs}{K_m + s + \frac{K_m}{K_i}p} \qquad (18)$$

The subscripts s and p refer to substrate and product conditions and D is the dispersion coefficient.

A more complex case in which the axial variation in v_{rw} cannot be neglected can be treated by dividing the total length of the HFER into a series of cells or compartments, as shown in Figure 2a. In each of the cells the radial velocity does not change with z and the simplifications already discussed can be applied to each cell. In this case, however, the lumen cells will each have different concentrations due to differing performances of the sponge cells and also the effect of flow from the lumen cells upstream. This complication must be accounted for in the boundary conditions associated with the concentration distribution equations and requires that the solution for each cell proceed from that end of the HFER where the lumen flow is zero. For cocurrent flow, this means that solution must begin from the reactor inlet.

To arrive at suitable boundary conditions for the reaction region, we adopt an approach similar to that of Ramkrishna and Amundson (1974). The concept involved can best be described by Figure 2b, which shows that each cell of the HFER is represented by a stirred tank connected to an axial dispersion plug-flow reactor, which is in turn connected in series in the radial direction of the HFER to a second stirred tank. All the second tanks again are connected in series in the axial direction of the HFER to represent the lumen region where the overall flow is plug flow without axial dispersion. For each cell, the uniform concentrations in the shell and lumen regions are well represented by the well-mixed stirred tanks. This schematic representation of the backflush HFER also permits the boundaries between the sponge region and the lumen to be open, that is, allow dispersion to take place there to account for any effect the fluid from a lumen cell may have on the enzymatic reaction in the sponge layer.

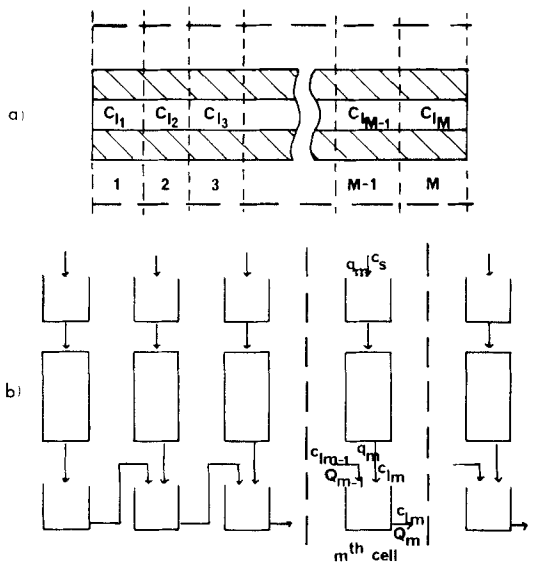

Figure 2a. Separation of HFER into *M* cells.
b. General model for a backflush HFER.

Consider the mth cell shown in Figure 2b. The volumetric flow rate of fluid from the shell is q_m with concentrations s_s and p_s in the shell. To save space, both concentrations are represented as c_s. Similarly, $c_{\ell m}$ represents either $s_{\ell m}$ or $p_{\ell m}$, etc. The same convention is applied later to Eqs. 19–23. The concentrations in the lumen are $s_{\ell m}$ and $p_{\ell m}$ and, because of continuity, these concentrations must be equal to the concentrations at the inner membrane wall. Q_{m-1} and Q_m are the volumetric flow rates entering and leaving the mth lumen cell, with corresponding concentrations being $c_{\ell m-1}$ and $c_{\ell m}$, respectively. The cross-sectional area of the sponge layer is X_{sm} at the shell wall and $X_{\ell m}$ at the lumen wall. Because of the definition of the positive radial direction, q_m is negative.

A mass balance at the inlet to the sponge region yields

$$qc_s - qc|_{r_o} + D_c X_s \left.\frac{dc}{dr}\right|_{r_o} = 0 \qquad (19)$$

where c refers to either the substrate or product concentration, and the subscript m is assumed throughout. Hence, recognizing that $q = v_{rw}X_s$, we have the boundary condition at $r = r_o$ as

$$\left.\frac{dc}{dr}\right|_{r_o} = -\frac{v_{rw}}{D_c}(c_s - c|_{r_o}) \qquad (20)$$

Similarly, at the exit of the sponge layer:

$$Q_{m-1}c_{\ell_{m-1}} + qc|_{r_i} - (q + Q_{m-1})c_\ell + D_c X_\ell \left.\frac{dc}{dr}\right|_{r_i} = 0 \qquad (21)$$

where $Q_{m-1} = 0$, for only one cell or for the first cell. Thus, for $m = 1$,

$$\left.\frac{dc}{dr}\right|_{r_i} = 0 \qquad (22)$$

Otherwise

$$\left.\frac{dc}{dr}\right|_{r_i} = \frac{-Q_{m-1}}{D_c X_\ell}(c_{\ell_{m-1}} - c|_{r_i}) \qquad (23)$$

It should be noted that the boundary conditions, Eqs. 20 and 23, become the Danckwert boundary conditions if $Q_{m-1} = 0$.

The equations and boundary conditions describing concentration distribution in the backflush HFER are put into dimension-

less form by introducing the dimensionless variables:

$$x \triangleq \frac{(r - r_i)}{(r_o - r_i)}; \quad p^* \triangleq \frac{p}{s_s}; \quad s^* \triangleq \frac{s}{s_s} \tag{24}$$

to obtain

$$\frac{d^2s^*}{dx^2} + \gamma(x)Pe_{1s}\frac{ds^*}{dx} - \Omega_s \frac{s^*}{\frac{K_m}{s_s} + s^* + \frac{K_m}{K_i}p^*} = 0 \tag{25}$$

$$\frac{d^2p^*}{dx^2} + \gamma(x)Pe_{1p}\frac{dp^*}{dx} + \Omega_p \frac{s^*}{\frac{K_m}{s_s} + s^* + \frac{K_m}{K_i}p^*} = 0 \tag{26}$$

$$\frac{ds^*}{dx} = -Pe_{3s}\left(\frac{s_{\ell_{m-1}}}{s_s} - s^*\right), \quad x = 0 \tag{27}$$

$$\frac{dp^*}{dx} = -Pe_{3p}\left(\frac{p_{\ell_{m-1}}}{s_s} - p^*\right), \quad x = 0 \tag{28}$$

$$\frac{ds^*}{dx} = -Pe_{2s}(1 - s^*), \quad x = 1 \tag{29}$$

$$\frac{dp^*}{dx} = -Pe_{2p}\left(\frac{p_s}{s_s} - p^*\right), \quad x = 1 \tag{30}$$

where

$$Pe_{1c} \triangleq \left(1 - \frac{v_{rw}r_o}{D_c}\right); \quad Pe_{2c} \triangleq \frac{v_{rw}(r_o - r_i)}{D_c};$$

$$Pe_{3c} \triangleq \frac{Q_{m-1}(r_o - r_i)}{D_c X_\ell} \tag{31}$$

and

$$\gamma(x) \triangleq \frac{(r_o - r_i)}{x(r_o - r_i) + r_i}; \quad \Omega \triangleq \frac{kE(r_o - r_i)^2}{D_c s_s} \tag{32}$$

with the subscript c representing either s or p.

It is possible to greatly reduce the complexity of the model for concentration distribution, Eqs. 25–30, if the diffusion coefficients of the substrate and the product have the same value. In this case, a simple linear relation exists between the substrate and the product concentrations:

$$s^* + p^* = 1 + \frac{p_s}{s_s} \tag{33}$$

Hence we only need to solve either Eq. 25 or Eq. 26.

Experimental Method

Activity and stability of lactases

Four samples of lactase (β-D-galactosidase, EC 3.2.1.23), each derived from a different microbial source, were evaluated with respect to their activity and stability and their suitability for immobilization in the sponge layer of the membranes.

The activity of free lactase was assayed based on the lactase-catalyzed reaction,

$$\beta\text{-lactose} + H_2O \rightarrow \beta\text{-D-galactose} + \beta\text{-D-glucose}$$

and was performed under the following conditions:

Lactose concentration = 50 g/L (0.146 M)
Lactase concentration = 0.2 – 0.5 LAU/mL
Temperature = 37°C
Reaction time = 5 min
pH = 4.4 (sodium citrate buffer) for fungal lactase
pH = 6.5 (milk buffer) for yeast and bacterial lactases

where one LAU (lactose activity unit) is defined as the amount of lactase that releases 1 μmol of glucose per minute under the conditions listed above. The reaction was stopped by the addition of 1M NaOH. The amount of glucose produced was measured by the glucose oxidase/peroxidase method after neutralization of the sample. The protein contents of the lactase preparations were determined by the Biuret method. It is worthwhile to mention that 150 ppm of benzalconium chloride (50% active) was added to the buffers to retard microbial growth. All the lactose solution used was prepared from anhydrous β-lactose (P-L Biochemicals).

The stability of free lactases was evaluated by mixing each enzyme sample with appropriate buffer to give a 10 mL solution containing about 20 mg of protein in sealed container. The lactase solutions were then placed in an incubating oven and maintained at 37°C for three days before assay for remaining activity.

A stirred ultrafiltration cell (Amicon, model 202) was used, in conjunction with a number of flat XM50 and PM10 membranes (Amicon, MW cutoff 50,000 and 10,000, respectively), to study the stability of lactases immobilized in the sponge layer of the membranes. The flat membranes were made of the same material and had the same structure as the corresponding hollow fibers, but could be removed easily for examination.

For reasons to be discussed later, the fungal lactase was eventually chosen in this work as the enzyme for immobilization in the HFER's. Hence the effect of pH and temperature on the activity of this lactase was studied. Furthermore, the kinetic parameters of the fungal lactase were also determined by analyzing the initial rate data, as well as by the progress curve data method. The progress curve tests were conducted at 35.5°C and pH 4.4 for initial lactose concentrations ranging between 47 and 162 g/L. The glucose content of the samples was determined using a glucose analyzer (Yellow Spring, model 27) after approximate neutralization of the samples with 1M HCl. Corrections were made for dilutions and the presence of galactose, which is also registered by the analyzer. Experimental procedures for the initial rate studies were similar to those of the progress curve tests except that temperatures of 35, 45, and 55°C were used.

Enzyme loading

A hollow-fiber cartridge (Amicon H1P5) containing PM5 hollow fibers was eventually chosen for use in this work to investigate the optimal means of loading the fungal lactase to the

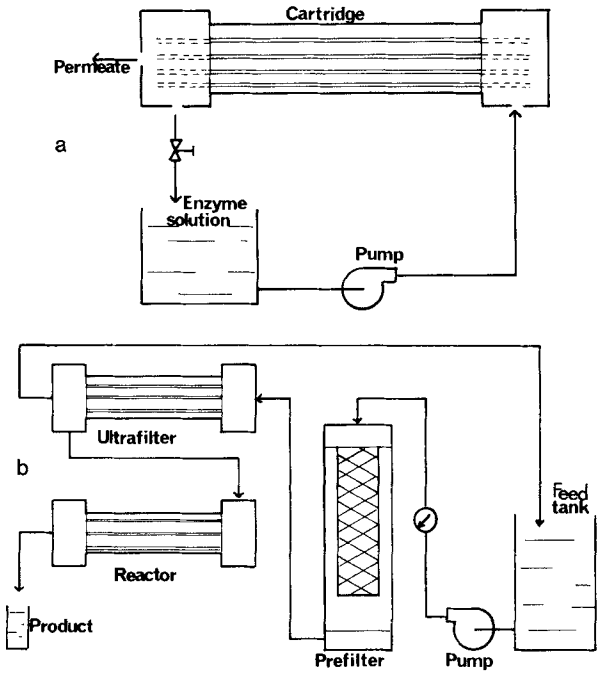

Figure 3a. Experimental setup for enzyme loading. b. Backflush HFER system.

spongy region of the hollow fibers. The experimental setup is illustrated in Figure 3a. During the preliminary trials, it was noted that the use of high hydrostatic pressures (e.g., greater than 70 kPa) more often resulted in enzyme gelling and fiber breakage, due to the subsequent rapid rise in pressure needed to maintain the same flow rate. This also caused washing back of the enzyme into the cartridge shell, once the high-pressure differential was removed. Furthermore, although loading time was reduced, high pressure did not result in higher enzyme loading. On the contrary, mild loading pressure resulted in a more complete immobilization of the lactase in the fiber sponge.

With these observations in mind, the following loading procedure, which was found to be reproducible and to cause no detectable presence of lactase in the cartridge shell surrounding the fiber bundle, was developed and used throughout this work:

1. Drain clean cartridge and fill sponge side with cold ultrafiltered sodium citrate buffer. Allow to stand for a half-hour and ensure no air bubbles in shell.

2. Pump cold ultrafiltered sodium citrate buffer through fiber lumen at a flow rate of 15 mL/min for 5 min, ensuring that there is a small flow from shell exit.

3. Dissolve the required amount of enzyme in 50 mL cold ultrafiltered citrate buffer and pump it to the shell side of the cartridge at a flow rate of about 10 mL/min. Recirculate enzyme solution from shell exit port to feed tank and leave lumen exit port open for 10 min.

4. Reduce flow rate and partially close shell-side exit to allow a flow rate of about 2 mL/min out of both the shell and lumen exits. Do not allow the pressure at the inlet of the cartridge to exceed 25 kPa. Collect filtrate.

5. After 1 h gradually close shell exit port, reducing flow rate to ensure that the shell inlet pressure is between 15 and 20 kPa.

6. Continue for 3 h, gently opening shell-side exit for 5 min every half-hour and refilling feed tank with filtrate as necessary.

7. Slowly drain shell and keep fluid for determination of enzyme content. Immediately refill shell with fresh, cold, ultrafiltered and buffered lactose solution, ensuring that no air bubbles are entrapped. Place reactor in position in water bath and introduce buffered lactose feed.

Extremely high enzyme loading density can be achieved simply by increasing the concentration of enzyme in the shell solution during loading or by repetitive backflushing. Once loaded and used, the cartridge may be cleaned for reloading. This was done by flushing the cartridge in ultrafiltration mode first with distilled water at a pressure differential of about 100 kPa, then with 500 mL 0.01M HCl, and finally with 1 L sodium citrate buffer. The acid ensures that any protein left in the cartridge is deactivated, and since the buffer contains benzalconium chloride as a bactericide, the cartridge may be stored under refrigeration for long periods without the possibility of bacterial contamination.

Reactor operation

A schematic illustration of the setup of the hollow-fiber enzymatic reactor system is shown in Figure 3b. The hollow-fiber cartridge (Amicon H1P5) used as the reactor was operated with the shell exit port closed. Preliminary runs had indicated that recirculation of the shell-side fluid resulted in lactase appearing in the shell, with significant reaction in that region, while samples taken from the shell during runs with the shell exit closed revealed no lactase.

During an experiment, the reactor, ultrafilter, prefilter, and the feed tank were all maintained at the required constant temperatures (35, 45, and 55°C) by being placed in a water bath. Under the experimental conditions there was no detectable pressure drop axially along the length of the shell.

The flow rate entering and leaving the reactor was measured by weighing the amount of product collected in a given time. The flow rates used in this study ranged from 0.4 to 15 mL/min, which corresponded to superficial velocities through the membrane wall of between 0.06 and 2.4 μm/s.

Since the immobilized lactase exhibited a high degree of stability, it was possible for a number of runs with the same enzyme loading and feed concentration to be performed without the need to clean the reactor and reload the enzyme. However, never were more than five runs performed with only one loading, and the total period over which these were conducted did not exceed six hours.

Results and Discussion

Evaluation and selection of lactases for immobilization

Shown in Table 1 are the activity and stability data obtained in this work for free lactases from fungal, yeast, and bacterial sources. The specific activity of the enzyme is a much more important indicator of its suitability for use in an immobilized enzyme reactor than the activity of the enzyme preparation per unit volume or weight of the sample. In addition to having the highest specific activity, the fungal lactase tested here also retained 100% of its original activity after three days of storage at 37°C. The bacterial lactase tested retained less than 10% of its original activity, while the yeast lactases also showed sub-

Table 1. Activity and Stability of Lactases Tested

Source	Activity	Protein Content	Specific Activity LAU/mg Protein	Frac. Orig. Activity Remaining
A. niger[1]	6,500 LAU/g	0.07 mg/mg	92.8	1.00
K. lactis[2]	1,950 LAU/mL	22.6 mg/mL	86.2	0.72
K. fragilis[3]	1,670 LAU/mL	19.6 mg/mL	85.2	0.78
E. coli[4]	46,000 LAU/g	0.91 mg/mg	50.5	<0.1

1. Lactase N, donated by GB Fermentation Industries
2. Maxilact L 2000, donated by GB Fermentation Industries
3. Lactozym 1500 L, donated by Novo Industries
4. Lactase B, from Sigma Co.

stantial deactivation. The bacterial lactase tested here was deleted from the list of lactase candidates for further work due to its poor stability.

In the process of evaluating immobilized lactases, it was found that significant enzyme leakage occurred through the XM50 membrane (MW cutoff 50,000). On the other hand, no fungal lactase leaked through the PM10 membrane and only a small amount of yeast enzyme leakage was detected toward the end of the experiments. Enzyme leakage was detected by noting a change in permeate glucose concentration with time upon storage.

The amount of protein recovered from the PM10 membrane at the end of each ultrafiltration cell experiment indicated that the lactases were retained by the membrane, perhaps by adsorption. The presence of lactase in the membrane was confirmed by the significant lactase activity that the membrane retained. Similar observations of adsorption by membranes have been reported before. Korus and Olson (1977) observed a strong adsorption of blue dextran by PM10 hollow fibers. Kohlwey and Cheryan (1981) reported that PM10 fibers adsorbed orthonitrobiphenyl to the extent of at least 80 mg/m^2 membrane. Waterland et al. (1975) found that a bacterial lactase was adsorbed by XM50 fibers but could be removed in inactive form by elution with 0.1M HCl.

The adsorption by the membrane appeared to be detrimental to the performance of the immobilized yeast lactases. This was reflected by the fact that the permeate glucose concentration for the fungal lactase remained steady between 39 and 42% conversion after the first two hours but the conversion for yeast lactases never exceeded 5%. It is possible that the adsorption is related to a group or subunit of the enzyme molecule that is near or associated with the active site of yeast lactases but distinct from the active site of fungal lactase. A number of workers (Kohlwey and Cheryan, 1981; Korus and Olson, 1977) suggested pretreating hollow fibers with bovine serum albumin to prevent deactivation of various enzymes upon contact with the membrane. In this work it was found that pretreatment of the ultrafiltration cell membrane with 10 mg milk protein, either β-lactoglobulin or α-lactoalbumin, greatly improved the activity of the yeast lactases, although it did not enhance their stability.

From the point of view of immobilizing the lactases in the spongy region of hollow fibers, the yeast lactases do not appear particularly suitable. The relatively poor stability makes their use commercially impractical. Lowering the reaction temperature will increase the stability of the enzyme but at the expense of decreasing the indicated activity of the enzyme. In addition, the protein pretreatment of the membrane that would be required if yeast lactases were used would reduce the amount of enzyme that could be loaded in the reactor. Thus, of the four sample lactases tested, the one form *A. niger* was chosen for use in the rest of this work.

Having determined that the *A. niger* lactase was the most suitable, based on work conducted on separate flat membranes, it was necessary to confirm this selection for hollow-fiber cartridges. Indeed it was found that the Amicon cartridge with PM10 fibers did not retain 100% of the fungal lactase loaded on them in backflush flow mode. For this reason, it was decided to use an Amicon cartridge (H1P5) with PM5 fibers (MW cutoff 5,000), which did totally retain the enzyme, as the backflush HFER of this work.

Tests were also conducted which indicated that galactose, glucose, and lactose were not adsorbed by either the active membrane or the spongy layer of the hollow fibers.

Kinetic properties of Aspergillus niger *lactase used*

The results of the pH and temperature studies on the *A. niger* lactase reveal that the lactase has a broad range of pH tolerance with an optimum (at 37°C) of about 4.4, and the temperature at which maximum activity (at pH 4.4) is displayed is 60°C. An Arrhenius plot of the temperature effect data gives an activation energy of 28.6 kJ/mol for the fungal lactase, which is a typical value for most enzymatic reactions.

The initial rate data were analyzed using a nonlinear regression routine and assuming a rate expression with competitive inhibition by β-galactose, Eq. 18. The values of the kinetic parameters associated with the rate expression, k, K_i, and K_m, were determined and are tabulated in Table 2.

The progress curve data were analyzed using a linear plot obtained by rearrangement of the rate expression in integrated form. Kinetic parameters estimated by this method are also presented in Table 2 and were found to be quite close to those obtained by the initial rate method for a comparable temperature. The results confirm that the competitive production inhibition rate expression assumed is valid and that the high values (30 to 80) of the K_m/K_i ratio indicate very strong product inhibition. Furthermore, the degree of inhibition is lower at higher temperatures, where the lactase activity is higher.

Reactor performance

A total of more than 180 runs were conducted on the hollow-fiber reactor under the following operational conditions:

1. S_o = 146 mM (50 g/L), E_o = 2,216, 1,173, 501, 153, 22 mg
2. S_o = 29.2 mM (10 g/L), E_o = 2,196, 1,216, 483, 19 mg
3. S_o = 2.92 mM (1 g/L), E_o = 2,218, 1,199, 507, 156, 20 mg

Table 2. Kinetic Parameters of *A. niger* Lactase (pH 4.4)

Method	Temp. °C	K_m mM	K_i mM	k mol/g lactase
Progress curve	35.5	91 ± 30	1.1 ± 0.4	6.5 ± 0.7
Initial rate	35	95 ± 25	1.2 ± 0.3	6.8 ± 0.4
Initial rate	45	62 ± 15	1.5 ± 0.3	9.3 ± 0.5
Initial rate	55	91 ± 15	2.9 ± 0.4	14.9 ± 0.7

4. S_o = 5.85 mM (2 g/L), E_o = 2,208, 1,216, 498, 156, 20 mg

5. S_o = 1.46 mM (0.5 g/L), E_o = 2,203, 1,197, 502, 174, 21 mg

For each set of conditions, five different flow rates (0.4, 0.8, 2.0, 8.0, and 15.0 mL/min) were used, and except for the last two sets, three reaction temperatures (35, 45, and 55°C) were involved.

Enzyme loadings slightly higher than 2,200 mg were repeatedly obtained. At this high loading, conversions over 90% were common, even at 35°C and with feed substrate concentration S_o as high as 10 g/L, so long as the flow rate was reasonably low. High conversions at high flow rates were also possible, if dilute lactose feed was used. For instance, conversions in excess of 90% were attained with a feed of 1 g/L lactose at a flow rate of 40 mL/m^2 of active membrane surface, and conversions in excess of 85% (or 75%) were obtained with the same feed at flow rates five (or 50) times greater. This compared very favorably with the 20% conversion at flow rates of less than 20 mL/m^2 of active membrane surface that are typical for other type of HFER's using much more dilute feed streams.

Conversion data collected for all the runs were tabulated and plotted (Jones, 1983). Some representative results are presented in Figure 4, where X is fractional conversion of lactose and $kE\tau/S_o$ is a dimensionless residence time (DRT) whose value is inversely proportional to flow rate. The predicted responses of the hollow-fiber enzymic reactor behaving as an ideal plug-flow tubular reactor (PFTR) and an ideal continuous stirred-tank reactor (CSTR) are also shown as solid or dashed curves for comparison.

Even for the relatively simple situation of one cartridge in single-pass operation at constant pH and uniform temperature, the data clearly indicate the complexity of the relation between reactor performance, expressed as conversion, and enzyme loading, feed substrate concentration, flow rate, and reaction temperature. The need for a mathematical model to describe the reactor is obvious. In general, however, the conversion increases as enzyme loading and/or temperature increase and as flow rate is reduced. The effect of flow rate is more noticeable at lower feed substrate concentration.

It is worthwhile to note that all the data fall in the region of reactor performance between the two ideal extremes of a CSTR and a PFTR, although the reactor behaves more like a CSTR than a PFTR under most of the operating conditions studied here. At the highest feed lactose concentration (50 g/L, Figure 4a), the deviation from CSTR behavior is nearly negligible. In general, this deviation is more noticeable at higher flow rate and lower S_o, Figure 4b–4d.

The reactor behavior mentioned above may be explained by realizing that under the experimental conditions of this work the lactose solution creeps slowly and evenly through the sponge layer and the thin membrane of the fibers. Thus we are dealing with very low velocities, very small distances, and steep concentration gradients. As the flow rate becomes smaller and smaller, dispersion (mainly molecular diffusion) in the radial direction of the hollow fibers starts to play a dominant role and the reactor behavior approaches that of a CSTR. Similarly, at high S_o the concentration gradients across the sponge layer are higher than that at lower S_o. This magnifies the relative importance of molecular diffusion, making the reactor appear to behave more like a CSTR.

Applications of the model

We shall first discuss the application of the model to the H1P5 hollow-fiber cartridges used in this work.

In the process of deriving Eq. 2, it was relatively easy to obtain the following relation for axial pressure gradient in the shell region of the reactor:

$$\frac{dp_1}{dz} = \frac{\mu\alpha}{r_o^2} v_{z_{1m}}(z) \tag{34}$$

From Eq. 34, the maximum possible pressure gradient in the shell was estimated to be about 0.23 kPa · m^{-1}. This is a very small pressure gradient; hence, it is reasonable to assume that in most cases, unless the reactor is very long, the shell-side pressure is constant. The assumption of constant shell-side pressure was also supported by the observation that during all experiments the axial pressure drop in the shell of the Amicon H1P5 cartridge was never more than 1 cm of H_2O for flow rates up to 15 mL min^{-1} and enzyme loadings as high as 2.2 g.

The question of whether constant radial wall velocity is justifiable for the H1P5 cartridge can also be checked here. Let us arbitrarily specify that the radial wall velocity may be considered constant if there is less than a 5% difference in their two extreme values $v_{rw}(\ell)$ and $v_{rw}(0)$. By applying Eq. 14 and neglecting the effect of the epoxy seal, we obtain $v_{rw}(\ell)/v_{rw}(0) = \cosh\beta \leq 1.05$, which is true if $\beta^2 \leq 0.1$, that is, if

$$\frac{16\mu r_o A\ell^2}{r_i^4} \leq 0.1 \tag{35}$$

then Equation 35 can be used to define a maximum possible cell length within which the assumption of constant radial wall velocity is valid. However, this analysis is valid only if the conditions for constant shell pressure are also satisfied.

Using values experimentally determined in this work for the hollow fiber (Jones, 1983) it can be seen that the assumption of a constant v_{rw} is quite valid for the H1P5 cartridge, which is only about 0.15 m long. In this case the deviation in the radial wall velocity is less than 1% along the whole length of the reactor. Indeed, in this case the assumption of a constant v_{rw} is valid for a reactor up to 0.5 m long. Hence, all the previous discussion indicates that a single cell (i.e., $m = 1$) is adequate to describe the performance of the backflush HFER used in this work.

A computer program was developed (Jones, 1983) to solve the multiple-cell model, Eqs. 25–30, using the orthogonal collocation method (Villadsen and Michelsen 1978). However, only the results that are relevant to the H1P5 cartridge used are presented here. For the general case where $D_p \neq D_s$, at least eight interior collocation points are needed to ensure that the solution obtained does not vary at a level detectable with six significant figures from the solution that would be obtained using one more collocation point. No numerical stability problems were experienced in the use of the computer program, even when applied to multicell cases. Parameter sensitivity analysis of the computer model was also carried out and it was found that the model is relatively sensitive to the value of r_o and relatively insensitive to the value of r_e. Overall, the sensitivity analysis shows that small inaccuracies in parameter estimation can be tolerated by the model without significantly affecting the model prediction.

For the lactose/lactase system investigated a comparison be-

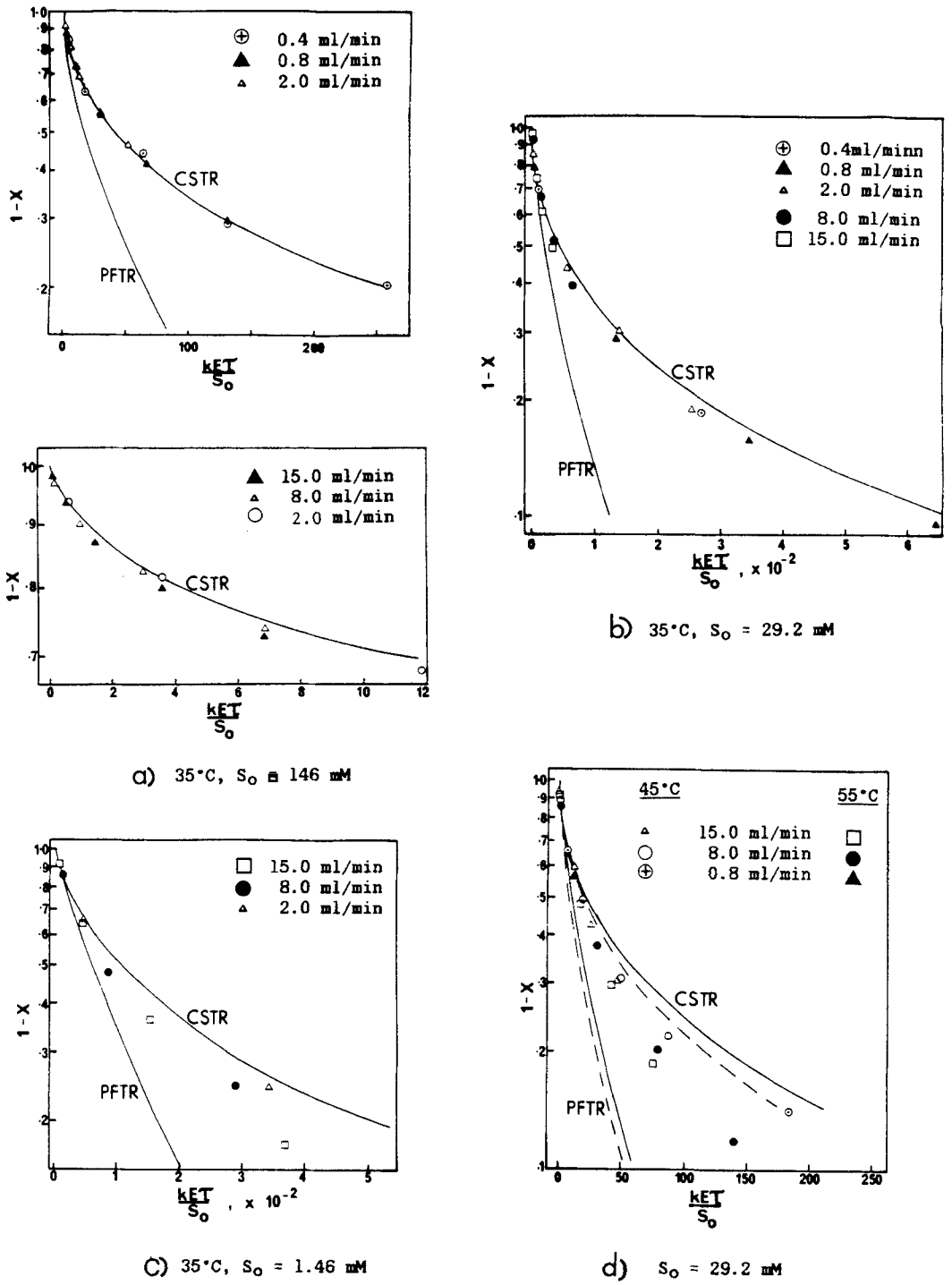

Figure 4. Fraction of lactose remaining vs. dimensionless residence time.
In (d): — 45°C; --- 55°C

tween the experimental results and the model predictions for flow rates of 2 and 15 mL/min and for various initial lactose concentrations ranging from 1.46 to 146 mM was made. Representative values of model parameters used are listed below:

$r_o = 4.75 \times 10^{-4}$ m
$r_i = 2.50 \times 10^{-4}$ m
$r_e = 6.25 \times 10^{-4}$ m
$v_{rw} = -2.35\ \mu\text{m} \cdot \text{s}^{-1}$
$D_s = 5.0 \times 10^{-10}\ \text{m}^2 \cdot \text{s}^{-1}$
$D_p = 7.0 \times 10^{-10}\ \text{m}^2 \cdot \text{s}^{-1}$
$s_s = 29.2$ mole $\cdot$ m^{-3}
$p_s = 0.0$ mole $\cdot$ m^{-3}
$K_m = 95.0$ mole $\cdot$ m^{-3}
$K_I = 1.2$ mole $\cdot$ m^{-3}
$k = 0.113$ mole $\cdot$ s^{-1} (kg enzyme)$^{-1}$
$E = 27.0$ kg $\cdot$ m^{-3}
$Pe_{3s} = 0.0$
$Pe_{3p} = 0.0$
$s_{\ell_{m-1}/s_s} = 1.0$
$p_{\ell_{m-1}/s_s} = 0.0$

Briefly, the radial wall velocity was determined from the feed flow rate to the reactor and the shell-side surface area of the hollow fibers. Kinetic parameters used were those determined for

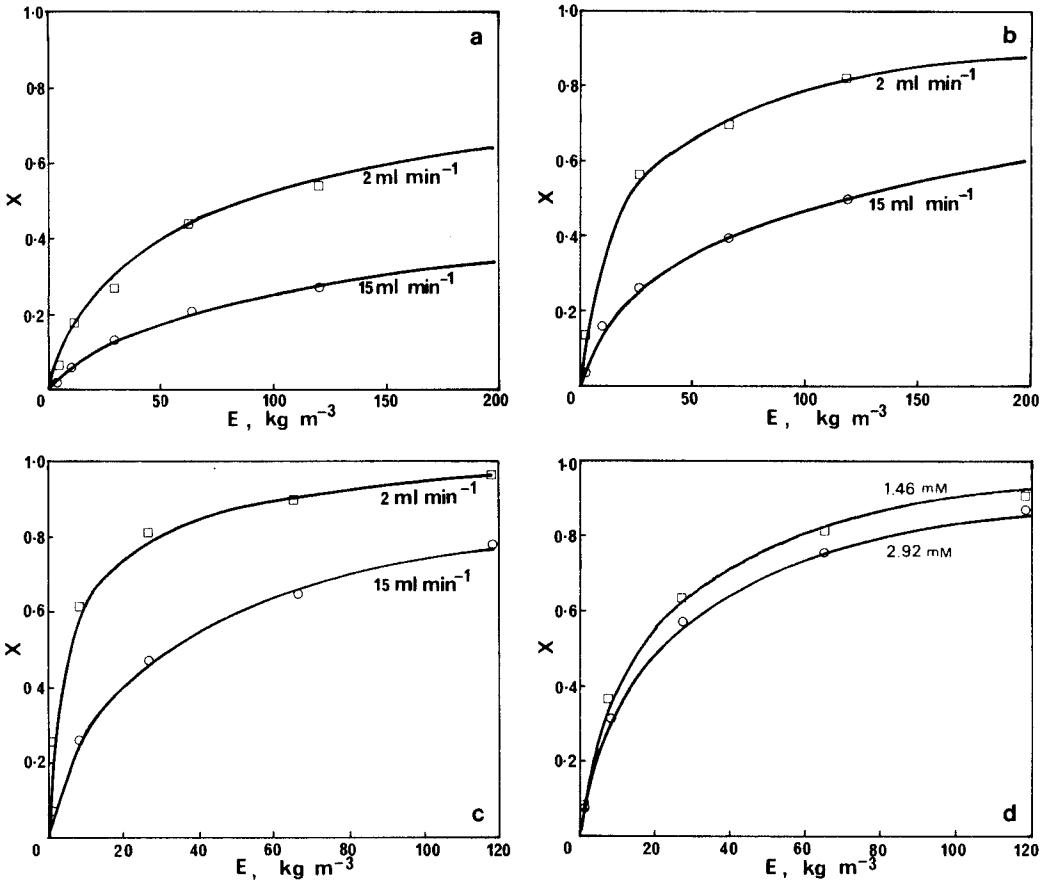

Figure 5. Lactose conversion X vs. lactase loading E at 35°C.

— Model predictions; □ ○ experimental data
a. S_o = 146 mM b. S_o = 29.2 mM
c. S_o = 5.85 mM d. 15 mL/min

free lactase, and the fiber geometry parameters were obtained from an electron microscope study of the hollow fibers conducted by Jones (1983). Molecular diffusion coefficients of the substrate and product were used for the dispersion coefficients D_s and D_p (Lee, 1981). As demonstrated by Figure 5, the agreement is in general excellent, and overall we have found that the behavior of a backflush HFER can be predicted accurately using the computer model developed.

Of significant importance is the fact that the values of the enzymatic kinetic parameters used in the model were those obtained experimentally for the (free) enzyme in a dilute aqueous environment. The excellent agreement between the experimental data and the model predictions suggests that the enzyme kinetics is not significantly altered during immobilization and operation. This, together with the fact that the performance of the reactor under practical conditions (high conversion, high substrate concentration, and complex reaction kinetics) can successfully be described mathematically, suggests that *a priori* design of a process-scale backflush HFER for a given purpose is possible, at least for the lactose/lactase system studied in this work.

At present the thickness of the sponge layer of a hollow fiber is controlled by the support role it plays for the thin membrane. Hence, there is little freedom in the choice of fiber thickness, although this situation is improving. On the other hand, fibers of greatly varying internal and external diameters are available. The model developed here can be used to determine fiber diameters, enzyme loadings, flow rates, and other factors that will yield the required performance for a backflush HFER.

Although the models and the computer program developed in this work have been written specifically for competitive product-inhibition type enzymatic reactions, they can easily be modified for application to other types of enzymatic reactions. Furthermore, the models in general should also be applicable to any membrane reactors operated in backflush mode, independent of the type of membranes involved, and most important, to any similar systems in which whole cells or organelles, instead of enzymes, are immobilized.

Notation

A = membrane coefficient
b = constant, Eq. 2c
c = concentration, either s or p
D = dispersion/diffusion coefficient
E = total enzyme concentration, enzyme loading
k = enzyme rate constant
K_i = product inhibition constant
K_m = Michaelis constant
ℓ = hollow fiber length
ℓ_s = fiber epoxy seal length
p = product concentration

P = pressure
Pe = Peclet number
P_{ex} = pressure at lumen exit
$\Delta p = P_1 - P_{ex}$
q = volumetric flow rate in sponge region
Q = volumetric flow rate in lumen
r = radial distance
r_e = equivalent fiber radius, Eq. 1
r_i = inner fiber radius
r_o = outer fiber radius
s = substrate concentration
S_o = initial substrate concentration
u = dimensionless axial velocity
V_r = radial velocity
V_{rw} = radial wall velocity
$\overline{V}_{rw}$ = area-averaged radial wall velocity
v_z = axial velocity
x = dimensionless radial distance, by Eq. 24
X = fiber wall surface area, lactose conversion
z = axial distance
z' = dummy variable

Greek letters

β = constant, Eq. 29a
$\gamma(x)$ = quantity, Eq. 32
$\delta = dP_3/dz$, Eq. 11
ϵ = reactor void fraction
ζ = dimensionless axial distance
η = constant, Eq. 2c
μ = viscosity
ν = kinematic viscosity
τ = residence time
ρ = fluid density
Ω = constant, Eq. 32

Superscript and subscripts

$*$ = dimensionless, Eq. 24
$c = s$ or p
j = 1, 2, or 3
ℓ = lumen region
m = area averaged or number of cell from reactor inlet
$m-1$ = $(m-1)$th cell
s = substrate or shell region
p = product
w = fiber wall
1 = shell region
2 = sponge region
3 = lumen region

Other symbols

$\triangleq$ = defined as

Literature Cited

Breslau, B. R., and B. H. Kilcullen, "Hollow-fiber Enzymatic Reactors—An Engineering Approach," *3rd Int. Conf. Enzyme Eng.*, Portland, OR (1975).

Dandavati, M. S., M. R. Doshi, and W. N. Gill, "Hollow-fiber Reverse Osmosis: Experiments and Analysis of Radial Flow Systems," *Chem. Eng. Sci.*, **30,** 877 (1975).

Doshi, M. R., W. N. Gill, and V. N. Kabadi, "Optimal Design of Hollow-fiber Modules," *AIChE J.*, **23**(5), 765 (1977).

Gill, W. N., and B. Bansal, "Hollow-Fiber Reverse-Osmosis Systems: Analysis and Design," *AIChE J.*, **19**(4), 823 (1973).

Jones, C. K. S., "Performance of a Radial Flow/Backflush Hollow-Fiber Enzymic Reactor," Ph.D. Thesis, Univ. Queensland, Australia (1983).

Kohlwey, D. E., and M. Cheryan, "Performance of a β-D-galactosidase Hollow-fiber Reactor," *Enzyme Microb. Technol.*, **3,** 64 (1981).

Korus, R. A., and A. C. Olson, "The Use of α-galactosidase and Invertase in Hollow-fiber Reactors," *Biotech. Bioeng.*, **19,** 1 (1977).

Lee, C. H., "Effects of Flow Dispersion on Hollow-fiber Module Performance," *Separ. Sci. Technol.*, **16**(1), 81 (1981).

Noda, I., and C. C. Gryte, "Mass Transfer in Regular Arrays of Hollow Fibers in Countercurrent Dialysis," *AIChE J.*, **25**(1), 113 (1979).

Pedersen, H., C. Horvath, and J. R. Bertino, "Immobilized Enzymes in Tubes and Hollow Fibers for Clinical Applications," *Enzyme Engineering 3*, Plenum, New York, 397 (1978).

Ramkrishna, D., and N. R. Amundson, "Stirred Pots, Tubular Reactors, and Self-Adjoint Operators," *Chem. Eng. Sci.*, **29,** 1353 (1974).

Robertson, C. R., A. S. Michaels, and L. R. Waterland, "Molecular Separation Barriers and Their Application to Catalytic Reactor Design," *Separ. Purif. Meth.*, **5**(2), 301 (1976).

Rony, P. R., "Multiphase Catalysis. II: Hollow-fiber Catalysts," *Biotech. Bioeng.*, **13,** 431 (1971).

Soltanieh, M., and W. N. Gill, "Review of Reverse-Osmosis Membranes and Transport Models," *Chem. Eng. Commun.*, **12,** 279 (1981).

Villadsen, J., and M. L. Michelsen, *Solution of Differential Equation Models by Polynomial Approximations*, Prentice-Hall, Englewood Cliffs, NJ (1978).

Waterland, L. R., A. S. Michaels, and C. R. Robertson, "A Theoretical Model for Enzymatic Catalysis Using Assymetric Hollow-fiber Membranes," *AIChE J.*, **20**(1), 50 (1974).

Waterland, L. R., C. R. Robertson, and A. S. Michaels, "Enzymatic Catalysis Using Assymetric Hollow-fiber Membranes," *Chem. Eng. Commun.*, **2,** 37 (1975).

Manuscript received Nov. 18 and Dec. 10, 1986 in two parts, and revision received Aug. 6, 1987.

See NAPS document no. 04549 for 15 pages of supplementary material. Order from NAPS c/o Microfiche Publications, P.O. Box 3513, Grand Central Station, New York, NY 10163. Remit in advance in U.S. funds only $7.75 for photocopies or $4.00 for microfiche. Outside the U.S. and Canada, add postage of $4.50 for the first 20 pages and $1.00 for each of 10 pages of material thereafter, $1.50 for microfiche postage.